

HOMOGENEOUS LOW-CRESTED STRUCTURES FOR BEACH PROTECTION IN CORAL REEF AREAS

Josep R. Medina¹, M. Esther Gómez-Martín¹, Patricia Mares-Nasarre¹, Mireille Escudero², Itxaso Odériz², Edgar Mendoza² and Rodolfo Silva²

In many countries, the health of the marine ecosystems and the sun-sand-sea tourism depend on the coral reefs, which have been retreating around the world during the last decades. Homogeneous Low-Crested Structures (HLCS), made of large rocks or pre-cast concrete units, can be placed to mimic the functions of beach protection and eventually serve as a refuge for species. HLCS is a type of multi-purpose green infrastructure which is functionally similar to conventional low-crested structures but have higher porosity and are more easily dismantled for re-use. Contrary to conventional low-crested structures, the functionality of HLCS protecting beaches depends on the selected placement grid; this paper describes physical and numerical placement tests on horizontal bottom used to characterize the layer coefficients of Cubipod[®] HLCS. The Bullet Physic Engine (BPE) numerical model used in the gaming industry, which is based on the rigid body method, is calibrated using the physical placement tests. The layer coefficients of Cubipod[®] HLCS measured in the physical placement tests were similar to those obtained with the BPE numerical model, which could be used to optimize placement grids of HLCS on specific sea bottom conditions. Finally, the influence of the placement grid of Cubipod[®] HLCS on the structure height, crest freeboard and wave transmission is analyzed.

Keywords: low-crested structures; coral reefs; armor units; Cubipod[®]; wave transmission; layer coefficient; placement grid; rigid body method;

INTRODUCTION

Climate change and other anthropic actions are affecting many coastal ecosystems. Sea level rise, ocean warming, ocean acidification generated by a rising concentration of CO₂ in the Earth's atmosphere, pollutants, over-fishing, and accidents are among the phenomena degrading coral reefs. In recent decades, it is estimated that coral reefs have been retreating at an annual rate of 1% to 2% in recent decades (see Rinkevich, 2014). This degradation reflects the impact of human perturbations on the biodiversity and coral reef functioning, resulting in poor health of the world's marine ecosystems. Furthermore, in some areas, the stability of nearby beaches depends on the state of health of coral reefs (see Ferrario et al., 2014).

It is well known that coral reefs are key elements for the stability of the marine ecosystems. In addition, coral reefs produce on average 2 kg/m² of calcium carbonate (CaCO₃) annually (see Hamylton et al., 2017) which means 1,000 m³/km² per year of biogenetic material for the constant nourishment of many sandy beaches around the world. In the short term, coral reefs protect adjacent beaches by reducing the wave energy that reaches the coastline, thus limiting the resultant coastal flooding and erosion occurring in storms (Silva et al., 2016). In the long term, coral reefs produce a significant amount of biogenic sand for the beaches and generate favourable conditions for the establishment of other ecosystems, such as seagrass fields.

Coral reefs are considered the most biologically diverse and economically valuable marine ecosystems in the world (see Mumby et al., 2007). In addition, many beaches close to coral reefs support valuable economic and social activities associated with sun, sea and sand tourism. However, the economic and social benefits of this kind of tourism often lead to further anthropic pressure in these regions, and thus to a progressive degradation of the coastal ecosystems.

Natural-based coastal protection solutions are gaining popularity (see Schoonees et al., 2019) to mitigate vulnerability to erosion and flooding as well as restore and preserve ecosystems. To protect sandy beaches in coral reef areas, Homogeneous Low-Crested Structures (HLCS) made of large rocks or pre-cast concrete elements are an option, in place of conventional Low-Crested Structures (LCS) with a core (see Odériz et al., 2018).

Conventional LCS (see Fig. 1a) are commonly used to protect beaches and can become the habitat of many species with a low visual impact. Detached breakwaters favour ecosystems connectivity between ecosystems; however, conventional LCS have a low-permeability core and require adequate quarries to provide the large rocks for the armour layer. HLCS are functionally similar to conventional LCS, but they have some key advantages in coral reef areas: (1) Concrete units can be used if large rocks are not

¹ Laboratory of Ports and Coasts, Universitat Politècnica de València, jrmedina@upv.es, mgomar00@upv.es, patmana@cam.upv.es, Spain

² Instituto de Ingeniería, Universidad Nacional Autónoma de México, mescudero@iingen.unam.mx, ioderizm@iingen.unam.mx, emendozab@iingen.unam.mx, rsilvac@iingen.unam.mx, México

available, (2) HLCS are easy to dismantle and the units can be re-used, (3) HLCS are highly porous structures with different light exposures, (4) The units are stable and adequate for coralline colonization and regeneration of coral reefs, (5) HLCS can attract and host different fish species, acting as an artificial reef, and (6) An HLCS can be a sustainable tourist attraction point. On the other hand, they have an inconvenience related to the use of concrete, which has higher carbon and energy footprints compared to large rocks quarried locally; however, this disadvantage is reduced when large rocks are not available at the construction site. HLCS should also be monitored after installation to control the colonization of species to guarantee a positive ecosystem evolution over time. Fig. 1b shows a cross section of a 3-layer Cubipod® HLCS.

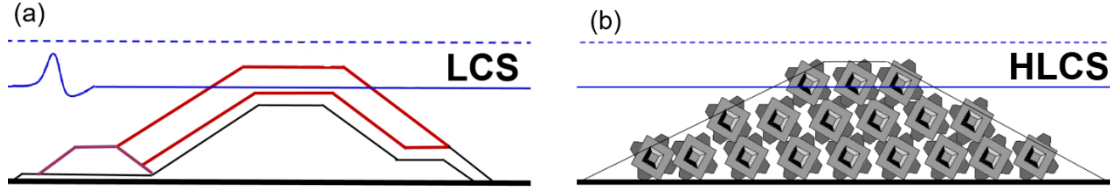


Figure 1. Cross sections of detached breakwaters: (a) Conventional LCS, and (b) 3-layer Cubipod® HLCS.

Depending on their location, space available and social urgency, HLCS may be considered multi-purpose green infrastructure, engineered ecosystems or ecologically enhanced hard infrastructure (see Silva et al., 2017). As a detached breakwater, an HLCS protects the coastline like a conventional LCS, but with a reduced environmental impact (clean construction, re-usable, easily dismantled, etc.). The elements of the HLCS offer a stable, highly porous structure, which provides a range of different light intensities between the elements, favouring local biodiversity and marine ecosystem restoration. An HLCS mimics the wave energy control provided by a coral reef and may restore habitats and enhance ecosystem services. A prototype installation in the Caribbean is planned to test this hypothesis (see Odériz et al., 2018). This paper provides some engineering criteria for the design of Cubipod® HLCS for typical Caribbean wave climate conditions, focusing on the estimation of structure height and crest freeboard related to the placement grid.

2D PHYSICAL TESTS

1-layer, 3-layer and 5-layer Cubipod® HLCS were tested in the Institute of Engineering of the National University of Mexico (II-UNAM) to define the best configuration of elements in the placement grids for the HLCS (see Odériz et al., 2018). Nine series of 2D small-scale hydraulic stability tests were carried out at the II-UNAM wave flume (19.0x0.40x0.52 m) with two different scales (1/37.5 and 1/42.8). The coefficient of transmission, $C_t = H_{st}/H_{si}$, is the most relevant parameter to characterize the performance of detached breakwater to protect beaches; Medina et al. (2019) recommended Eqs. (1) to (3) to estimate the coefficient of transmission for the 1-layer, 3-layer and 5-layer Cubipod® HLCS tested at II-UNAM, named A1, C3 and B5, respectively.

$$C_t(A1) = 0.45 - 0.30 \left(\frac{R_c}{H_{si}} \right) \quad (1)$$

$$C_t(C3) = 0.60 - 0.35 \left(\frac{R_c}{H_{si}} \right) \quad (2)$$

$$C_t(B5) = \max \left[0.54; 0.54 - 0.40 \left(\frac{R_c}{H_{si}} \right) \right] \quad (3)$$

where C_t = coefficient of transmission, R_c = crest freeboard, and H_{si} = incident significant wave height. When comparing Eqs. (1) to (3) with Eq. (4) recommended by d'Angremond et al. (1996) for conventional LCS, Cubipod® HLCS showed higher coefficient of transmission than conventional LCS with a relatively impermeable core (see Medina et al., 2019).

$$C_t = -0.4 \left(\frac{R_c}{H_{si}} \right) + 0.64 \left(\frac{B}{H_{si}} \right)^{-0.31} \left(1 - e^{-\frac{I_{rpi}}{2}} \right) \quad (4)$$

where B = crest width, and I_{rpi} = Iribarren number using H_{si} and peak period (T_p). Fig. 2 compares the measured coefficient of transmission (full symbols) of A1 (black), C3 (blue) and B5 (red) Cubipod® HLCS to estimations given by Eqs. (1) to (3), and also compares to estimations given by Eq. (4) corresponding to conventional LCS (open symbols).

The beach protection offered by HLCS is related to energy dissipation and wave transmission. This is highly dependent on the crest freeboard; the higher the dimensionless crest freeboard, R_c/H_{si} , the lower the coefficient of transmission (see Fig. 2). Applying Eq. (1), 1-layer Cubipod® HLCS (A1) showed similar coefficients of transmission than those obtained by Eq. (4) for conventional LCS. 3-layer and 5-layer Cubipod® HLCS showed higher coefficients of transmissions than conventional LCS (Eq. (4)) when considering similar envelope profiles.

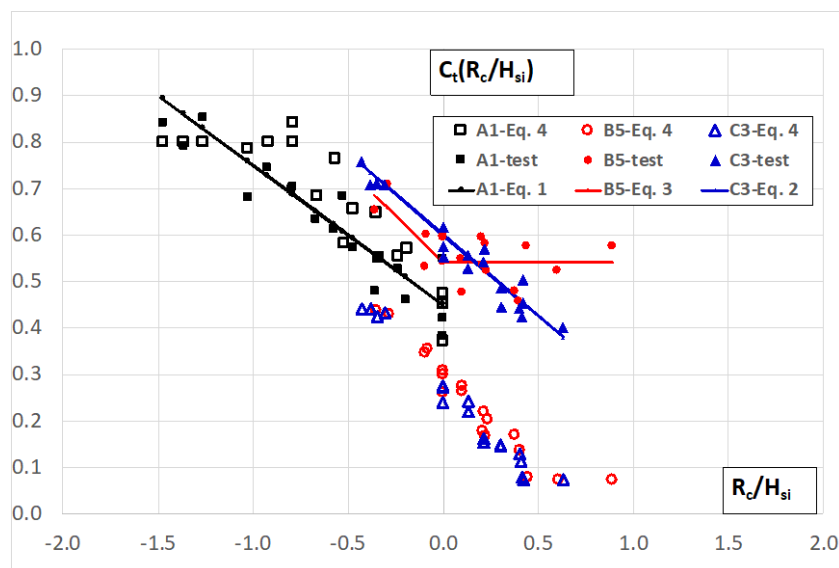


Figure 2. Observed coefficient of transmission C_t (full symbols) of Cubipod® HLCS compared to estimations given by Eqs. (1) to (3) and estimated C_t using Eq. (4) valid for conventional LCS.

Fig. 3 shows the squared of the coefficients of transmission, reflection and dissipation, which describe the proportion of incident energy that is transmitted, reflected and dissipated. Eq. (5) describes the conservation of energy in the 2D tests.

$$1 = C_t^2 + C_r^2 + C_d^2 \quad (5)$$

where $C_t=H_{st}/H_{si}$ and $C_r=H_{sr}/H_{si}$. The reflected energy and the dissipated energy increase with the dimensionless crest freeboard, R_c/H_{si} . As a result, the transmitted energy clearly decreases with increasing R_c/H_{si} . Therefore, an adequate design and construction of Cubipod® HLCS require the right estimation of the height of the structure which is directly related to the crest freeboard.

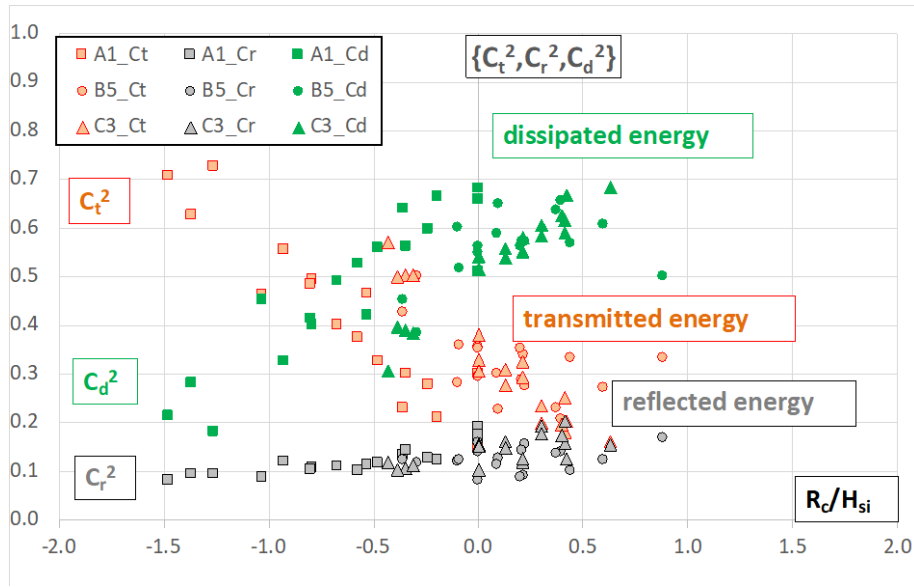


Figure 3. Proportion of incident wave energy given by C_t^2 (orange), C_r^2 (grey) and C_d^2 (green) as a function of the dimensionless crest freeboard for A1, C3 and B5 Cubipod® HLCS.

CREST FREEBOARD AND PLACEMENT GRID

The height of a conventional LCS and the corresponding crest freeboard can be easily adjusted at the construction site just by controlling the elevation of the core. On the other hand, the height and crest freeboard of an HLCS made of large rocks or pre-cast concrete units can only be modified through the number of layers and the placement grid.

Fig. 4 shows a scheme of the relationship between placement grid and height of the structure, and crest freeboard; the wider the placement grid, the lower the HLCS. The placement grid of an HLCS is relevant, not only for logistics and economic reasons but also for the protection function provided by the structure. The thickness of an armour layer, which is a secondary characteristic in conventional mound breakwaters, is relevant in HLCS because it affects the crest freeboard and wave transmission. Thus, clear criteria to estimate the layer thicknesses and the layer coefficients of Cubipod® HLCS as well as adequate approaches to guarantee the designed crest freeboard of both small-scale and prototype HLCS are required.

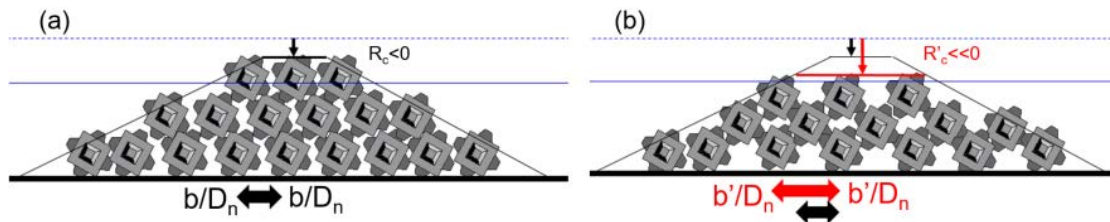


Figure 4. Two placement grids for a 3-layer Cubipod® HLCS: (a) higher R_c and (b) lower R_c .

Porosity describes the proportion of voids in a granular system. Although porosity is intuitive and easy to define, it is not so clear when applied to armour layers with randomly-orientated large units. Most engineering manuals, for given armour units, recommend specific layer coefficient and nominal porosity (k_Δ and $P\%$) which are directly related to the placing density, ϕ , given by Eq. 6 (see SPM, 1984).

$$\phi = n(k_\Delta)(1 - P\%) \left(\frac{\gamma_r}{W} \right)^{\frac{2}{3}} \quad (6)$$

where n =number of layers, k_Δ =layer coefficient, $P\%$ =nominal porosity, W =weight of the armour unit and γ_r =specific weight of the material of the unit (concrete or rock). The placing density is dimensional (e.g. units/m²); a more convenient parameter to measure the concrete consumption is the packing density, Φ . The dimensionless placing density is given by Eq. 7.

$$\Phi = (D_n^2)\phi = n(k_\Delta)(1 - P\%) \quad (7)$$

where $D_n=(W/\gamma_r)^{1/3}$ is the nominal diameter or equivalent cube size. Placing or packing densities have a clear physical meaning, but porosity and layer coefficient depend on each other because the product $(1-P\%) k_\Delta$ is the term used in Eqs. (6) and (7). Freens (2007) pointed out some misinterpretations caused by the use of different layer coefficients and corresponding porosities by different authors. As noted by Medina et al. (2010), $P\%=0.47$ with $k_\Delta=1.10$ in Eqs. (6) and (7) is equivalent to $P\%=0.42$ with $k_\Delta=1.00$; for a given number of layers and packing density, the criterion to define the layer coefficient, k_Δ , affects the nominal porosity.

For conventional mound breakwaters and randomly-placed units, it is not relevant the use of different criteria to define the layer coefficient, because the relevant term is $\{(1-P\%) k_\Delta\}$ and the recommended layer coefficient, k_Δ , for a specific armour unit is always published with the corresponding armour porosity, $P\%$. This is not the case for Cubipod® HLCS, because the layer coefficient of each layer not only affects the porosity and concrete consumption but also the structure height and crest freeboard of the structure. A clear criterion is needed to define the thickness of each layer applicable to both small-scale physical tests and prototype scale.

In this study, the methodology proposed by Keyser and Jacobs (2020) is used to estimate the layer thicknesses and the overall structure height of a Cubipod® HLCS. The placement tests of Keyser and Jacobs (2020) were conducted on horizontal bottom and analysed different rectangular and triangular placement grids characterized by the separation between units in the wave direction (a/D_n) and in the perpendicular direction (b/D_n). The triangular placement grid used by Odériz et al. (2018) for the physical tests described in the previous section is characterized by $a/D_n=1.58$ and $b/D_n=1.27$, very close to the equilateral triangle and $[(1-P\%) k_\Delta]=0.50$.

Squared plates, with side $2D_n$, were placed on top of each layer to measure the height of the structure using a laser distance meter mounted on a reference framework. Fig. 5 shows a general view of the measurement system; the placement grid is drawn on the floor and the small-scale units ($D_n(m)=0.038$) are placed by hand in their approximate X-Y position in the first layer. In the upper layers, they are placed on top of three (triangular grid) or four (rectangular grid) neighbouring units in the upper layers.



Figure 5. Measurement of layer thickness in the physical placement tests using a rectangular grid with $a/D_n=1.40$ and $b/D_n=1.30$ (Keyser and Jacobs, 2020)

The first layer thickness is the distance between two horizontal envelopes, the bottom and the plates. This thickness is determined by the geometry of the Cubipod® placed with random orientation on the floor; geometry and measurements gave similar results: $k_{\Delta 1}=1.30$. The layer thickness was defined as the distance between envelopes; the layer coefficients of the upper layers were lower than $k_\Delta=1.30$ because some parts of the Cubipod® units may be placed below the upper envelope of the bottom layer. Fig. 6 shows the measured layer coefficients for a triangular placement grid with $a/D_n=1.58$ and $b/D_n=1.27$.

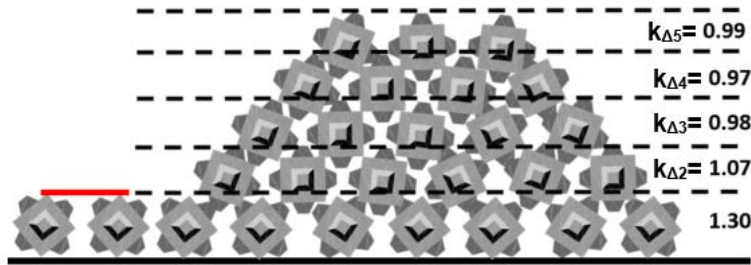


Figure 6. Layer coefficients corresponding to a triangular placement grid with $a/D_n=1.58$ and $b/D_n=1.27$

The layer coefficients depend on the placement grid; if a/D_n and b/D_n increases, $k_{\Delta j}$ decreases ($j>1$). Cubipod® HLCS require a precise characterization of the placement grid in small-scale tests and prototype to properly estimate three key factors: hydraulic stability, wave transmission and concrete consumption.

ANALYZING PLACEMENT GRIDS WITH A GAME ENGINE

Recently, Centi (2020) used the results of the above physical placement tests to calibrate a Bullet Physical Engine (BPE) for numerical placement tests of Cubipod® HLCS. The BPE is based on the use of the Newton's laws on rigid bodies. The numerical simulations used approximations with some parameters which may affect the results of the numerical placement:

1. Friction (μ). Ratio between tangential and normal forces, which depends on the type of material.
2. Bounciness (e). Restitution coefficient or ratio between final and initial velocity after collision.
3. Linear damping (d). Numerical coefficient to reduce linear velocities in time.
4. Angular damping (d_a). Numerical coefficient to reduce angular velocities in time.
5. Collision margin (CM). Minimum distance where collisions are considered.

Keyser and Jacobs (2020) used small-scale Cubipod® units ($D_n(m)=0.038$) for their physical placement tests while Centi (2020) used large Cubipod® units ($D_n(m)=1.07$, $W(t)=2.8$) for his numerical placement tests. After some sensitivity analysis, numerical simulations with Blender (2019) were carried out with null linear and angular damping ($d=d_a=0$), friction $\mu=0.8$, bounciness $e=0.01$ and collision margin $CM(m)=0.01$. To simulate the hand placement with a specific placement grid, Cubipod® units were placed randomly orientated in the first layer and released from a height of 0.2 m above the previous layer; all units from the same layer were placed or released simultaneously in the numerical placement tests. Fig. 7 shows a view of the numerical placement test corresponding to the second layer (blue units).

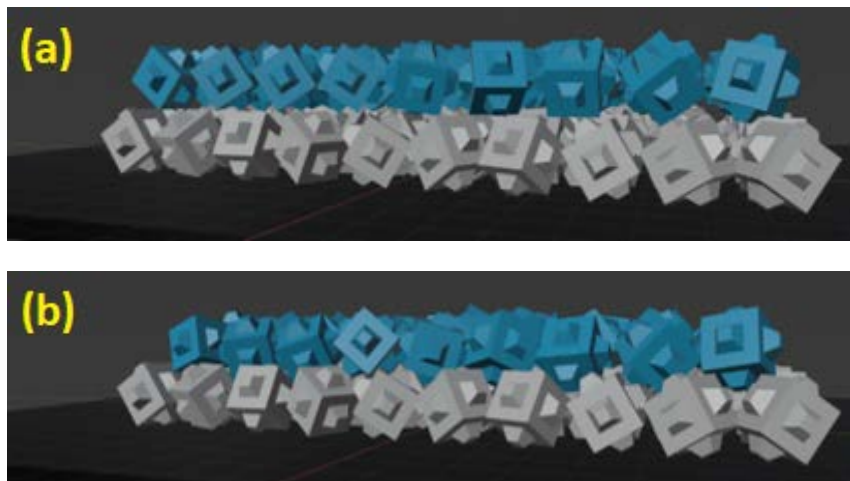


Figure 7. Numerical placement of the second layer (blue units): (a) before and (b) after releasing the Cubipod® units.

Fig. 8 shows an example of the numerical measurement system implemented by Centi (2020) similar to that used by Keyser and Jacobs (2020) in their physical placement tests shown in Fig. 5. The numerical

and physical placement tests showed similar layer coefficients for both rectangular ($a/D_n=1.40$ and $b/D_n=1.30$) and triangular ($a/D_n=1.58$ and $b/D_n=1.27$) placement grids, with differences lower than 5%. The repeatability tests described by Centi (2020) showed a Coefficient of Variation $CV \approx 1\%$ for both physical and numerical placement tests.

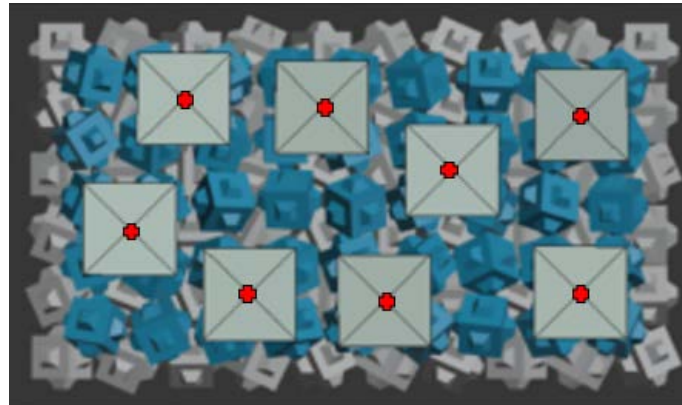


Figure 8. Measurement of layer thickness in the physical placement tests using a rectangular grid with $a/D_n=1.40$ and $b/D_n=1.30$ (Keyser and Jacobs, 2020).

Table 1 shows the measured layer coefficients measured in the physical tests (PT) and numerical tests (NT) with a rectangular placement grid ($a/D_n=1.40$ and $b/D_n=1.30$). Table 2 shows the layer coefficients corresponding to PT and NT with a triangular placement grid ($a/D_n=1.58$ and $b/D_n=1.27$). The repeatability results (Tables 1 and 2) with data given by Centi (2020) and Keyser and Jacobs (2020) showed a good agreement and a Coefficient of Variation $CV < 2.2\%$ for both physical and numerical placement tests.

The good agreement between the layer thicknesses of Cubipod® HLCS measured in the numerical and physical placement tests shows that with the BPE software is possible to estimate reasonably the structure height and crest freeboard of a Cubipod® HLCS in real conditions. For a realistic numerical simulation at prototype scale, a specific bathymetry and placement grid can be considered.

	Physical Placement Tests								Numerical Placement Tests				
	PT1	PT2	PT3	PT4	PT5	PT6	PTm	CV	PT1	PT2	PT3	PTm	CV
$k_{\Delta 1}$	1.31	1.32	1.31	1.32	1.31	1.32	1.32	0.4%	1.32	1.32	1.32	1.32	0.0%
$k_{\Delta 2}$	1.02	1.04	1.04	1.07	1.04	1.06	1.05	1.7%	1.09	1.09	1.09	1.09	0.0%
$k_{\Delta 3}$	0.93	0.95	0.93	0.94	0.95	0.91	0.94	1.6%	0.95	0.91	0.93	0.93	2.2%
$k_{\Delta 4}$	0.89	0.94	0.96	0.93	0.94	0.97	0.94	3.0%	0.95	0.96	0.92	0.94	2.2%
$k_{\Delta 5}$	0.91	0.95	0.87	0.94	0.88	0.92	0.91	3.5%	0.90	0.90	0.92	0.91	1.3%

	Physical Placement Tests										Numerical Placement Tests				
	PT1	PT2	PT3	PT4	PT5	PT6	PT7	PT8	PTm	CV	PT1	PT2	PT3	PTm	CV
$k_{\Delta 1}$	1.30	1.30	1.31	1.30	1.30	1.29	1.29	1.28	1.30	0.7%	1.31	1.31	1.31	1.31	0.0%
$k_{\Delta 2}$	1.07	1.08	1.05	1.07	1.07	1.07	1.09	1.08	1.07	1.1%	1.12	1.13	1.13	1.13	0.5%
$k_{\Delta 3}$	1.01	0.96	0.98	0.99	0.96	0.99	0.98	0.96	0.98	1.9%	1.00	0.99	1.01	1.00	1.0%
$k_{\Delta 4}$	0.95	0.99	0.98	0.97	0.97	0.97	0.99	0.93	0.97	2.1%	1.03	1.04	1.00	1.02	2.0%
$k_{\Delta 5}$	1.00	1.00	0.95	0.99	0.96	1.00	1.00	0.97	0.98	2.1%	1.00	0.98	1.00	0.99	1.2%

SUMMARY AND CONCLUSIONS

Conventional LCS are commonly used to protect beaches. However, LCS have low core permeability and adequate quarries are required to provide the large rocks for the armour layer. HLCS are functionally similar to conventional LCS but present some key advantages in coral reef areas: (1) concrete units can be used if large rocks are not available, (2) easy to dismantle with re-use of units, (3) highly porous structure with different light exposures, (4) adequate for coralline colonization and regeneration, (5) attraction and hosting different fish species, and (6) sustainable tourist attraction. An HLCS mimics the wave energy control provided by a coral reef and may restore habitats and enhance ecosystem services.

In order to mimic some of the hydrodynamic functions of coral reefs and allow the establishment of habitats, it is critical to characterize transmission, reflection and dissipation coefficients, as well as the porosity and roughness of the structures, and may integrate ecosystems with a low visual impact. To this end, nine series of 2D small-scale hydraulic stability tests were carried out at the II-UNAM wave flume with two different scales. Eqs. (1) to (3) can be used to estimate the coefficient of transmission for the 1-layer, 3-layer and 5-layer Cubipod® HLCS tested at II-UNAM. 3-layer and 5-layer Cubipod® HLCS showed higher coefficient of transmissions than a conventional LCS with a similar envelope profile. The reflected energy slightly increases with the dimensionless crest freeboard but energy dissipation caused by HLCS significantly increases with dimensionless crest freeboard; the transmitted energy clearly decreases with increasing dimensionless crest freeboard. An adequate design and construction of Cubipod® HLCS require the right estimation of the height of the structure which is directly related to the crest freeboard.

The height of a conventional LCS and the corresponding crest freeboard can be easily adjusted at the construction site just raising or lowering the core crest. On the contrary, the height and crest freeboard of HLCS made of large rocks or pre-cast concrete units can only be modified through the number of layers and the placement grid. The placement grid of HLCS is a relevant issue, not only for logistics and economic reasons but also for the functionality of the structure protecting beaches. The layer coefficients of a HLCS not only affects the porosity and concrete consumption but also the structure height and crest freeboard. A clear criterion is proposed in this paper to define the thickness of each layer applicable to both small-scale physical tests and prototype scale.

In this study, the methodology and results proposed by Keyser and Jacobs (2020) and Centi (2020) are used to estimate the layer thicknesses and structure height of Cubipod® HLCS in physical and numerical placement tests carried out on horizontal bottom. Different rectangular and triangular placement grids were studied, including the previous triangular placement grid used at II-UNAM for the 2D physical tests. In the physical tests, squared plates with side $2D_n$ were placed on top of each layer to measure the height of the structure. A laser distance meter mounted on a reference framework was used for the physical tests and a Bullet Physical Engine (BPE) was used for the numerical placement tests. The simulations performed in this study with the BPE have three parameters: friction $\mu=0.8$, bounciness $e=0.01$, and collision margin $CM(m)=0.01$ with no damping.

The numerical and physical placement tests showed similar layer coefficients for both rectangular ($a/D_n=1.40$ and $b/D_n=1.30$) and triangular ($a/D_n=1.58$ and $b/D_n=1.27$) placement grids, with differences lower than 5%. The repeatability tests showed a Coefficient of Variation $CV<2.2\%$ for both physical and numerical placement tests. For real conditions with a given bathymetry and a specific placement grid for construction at prototype scale, the good agreement between the layer thicknesses of Cubipod® HLCS measured in the numerical and physical placement tests makes the BPE software a feasible approach to estimate the structure height and crest freeboard of Cubipod® HLCS.

ACKNOWLEDGMENTS

The authors wish to acknowledge the financial support of the Spanish *Ministerio de Ciencia, Innovación y Universidades* (Grant RTI2018-101073-B-I00), and Riccardo Centi, Karel De Keyser and Elias Jacobs, for designing and conducting the numerical and physical placement test in their master's theses.

REFERENCES

- Blender, 2019. Blender 2.80 Reference Manual. Available at <https://www.blender.org/> and visited in January 2020.
- Centi, R., 2020. Placement of homogeneous artificial mound breakwaters using a game engine. MSc. thesis, University of L'Aquila (ITA), September 2020.
- De Keyser, K., Jacobs, E., 2020. La literature review on low-crested and submerged structures. MSc. thesis, Ghent University (BE), June 2020.
- Ferrario, F., Beck, M.W., Storlazzi, C.D., Micheli, F., Shepard, C.C. Airoidi, L., 2014. The effectiveness of coral reefs for coastal hazard risk reduction and adaptation. *Nature Communications*, 5 (3794), 98-101.
- Frens, A.B. 2007. *The impact of placement method on Antifer-block stability*. M.Sc. thesis, Delft University of Technology (NL), May 2007.
- Hamylton, S.M., Duce, S., Vila-Concejo, A., Roelfsema, C.M., Phinn, S.R., Carvalho, R.C., Shawe, E.C., and Joyce, K.E., 2017. Estimating regional coral reef calcium carbonate production from remotely sensed seafloor maps. *Remote Sensing of Environment*, 201(2017): 88-98.

- Medina, J.R., Gómez-Martín, M.E., Corredor, A., 2010. Influence of armour unit placement on armour porosity and hydraulic stability. *Proc. 32nd Int. Conf. on Coastal Engineering*, ASCE, 1(32), structures.41. doi:10.9753/icce.v32.structures.41.
- Medina, J.R., Gómez-Martín, M.E., Mares-Nasarre, P., Odériz, I., Mendoza, E., Silva, R., 2019. Hydraulic performance of homogeneous low-crested structures, *Proc. of the Coastal Structures Conference 2019*, Bundesanstalt für Wasserbau (BAW), Karlsruhe (GE), 60-68.
- Mumby, P.J., Hastings, A., Edwards, H.J., 2007. Thresholds and the resilience of Caribbean coral reefs. *Nature*, 450, 98–101.
- Odériz, I., Mendoza, E., Silva, R., Medina, J.R., 2018. Hydraulic performance of a homogeneous Cubipod low-crested mound breakwater. *Proc. of the 7th International Conference on the Application of Physical Modelling in Coastal and Port Engineering and Science (Coastalab18)*, (in press).
- Rinkevich, B., 2014. Rebuilding coral reefs: does active reef restoration lead to sustainable reefs? *Current Opinion in Environmental Sustainability*, 7 (2014), 28–36.
- Schoonees, T., Gijón-Mancheño, A., Scheres, B., Bouma, T. J., Silva, R., Schlurmann, T., Schüttrumpf, H., 2019. Hard Structures for Coastal Protection, Towards Greener Designs. *Estuaries and Coasts*. <https://doi.org/10.1007/s12237-019-00551-z>
- Silva, R., Lithgow, D., Esteves, L.S., Martínez, M.L., Moreno-Casasola, P., Martell, R., Pereira, P., Mendoza, E., Campos-Cascaredo, A., Grez, P.W., Osorio, A.F., Osorio-Cano, J.D., Rivillas, G.D., 2017. Coastal risk mitigation by green infrastructure in Latin America. *Proc. of the Institution of Civil Engineers-Maritime Engineering*, 170 (2), 39-54.
- Silva, R., Mendoza, E., Mariño-Tapia, I., Martínez, M.L., Escalante, E., 2016. An artificial reef improves coastal protection and provides a base for coral recovery. *Journal of Coastal Research*, 75, 467-471.
- SPM. 1984. *Shore Protection Manual*, U.S. Army Corps of Engineers, Waterways Experiment Station, Coastal and Hydraulics Laboratory, Vicksburg, MS.